

Correlative imaging across microscopy platforms using the fast and accurate relocation of microscopic experimental regions (FARMER) method

Toan Huynh, Matthew K. Daddysman, Ying Bao, Alan Selewa, Andrey Kuznetsov, Louis H. Philipson, and Norbert F. Scherer

Citation: [Review of Scientific Instruments](#) **88**, 053702 (2017); doi: 10.1063/1.4982818

View online: <http://dx.doi.org/10.1063/1.4982818>

View Table of Contents: <http://aip.scitation.org/toc/rsi/88/5>

Published by the [American Institute of Physics](#)



Correlative imaging across microscopy platforms using the fast and accurate relocation of microscopic experimental regions (FARMER) method

Toan Huynh,^{1,a),b)} Matthew K. Daddysman,^{2,a)} Ying Bao,³ Alan Selewa,² Andrey Kuznetsov,⁴ Louis H. Philipson,⁴ and Norbert F. Scherer^{1,2,3,c)}

¹Department of Chemistry, University of Chicago, Chicago, Illinois 60637, USA

²Institute for Biophysical Dynamics, University of Chicago, Chicago, Illinois 60637, USA

³James Franck Institute, University of Chicago, Chicago, Illinois 60637, USA

⁴Department of Medicine, University of Chicago, Chicago, Illinois 60637, USA

(Received 19 January 2017; accepted 18 April 2017; published online 15 May 2017)

Imaging specific regions of interest (ROIs) of nanomaterials or biological samples with different imaging modalities (e.g., light and electron microscopy) or at subsequent time points (e.g., before and after off-microscope procedures) requires relocating the ROIs. Unfortunately, relocation is typically difficult and very time consuming to achieve. Previously developed techniques involve the fabrication of arrays of features, the procedures for which are complex, and the added features can interfere with imaging the ROIs. We report the Fast and Accurate Relocation of Microscopic Experimental Regions (FARMER) method, which only requires determining the coordinates of 3 (or more) conspicuous reference points (REFs) and employs an algorithm based on geometric operators to relocate ROIs in subsequent imaging sessions. The 3 REFs can be quickly added to various regions of a sample using simple tools (e.g., permanent markers or conductive pens) and do not interfere with the ROIs. The coordinates of the REFs and the ROIs are obtained in the first imaging session (on a particular microscope platform) using an accurate and precise encoded motorized stage. In subsequent imaging sessions, the FARMER algorithm finds the new coordinates of the ROIs (on the same or different platforms), using the coordinates of the manually located REFs and the previously recorded coordinates. FARMER is convenient, fast (3–15 min/session, at least 10-fold faster than manual searches), accurate ($4.4 \mu\text{m}$ average error on a microscope with a 100x objective), and precise (almost all errors are $<8 \mu\text{m}$), even with deliberate rotating and tilting of the sample well beyond normal repositioning accuracy. We demonstrate this versatility by imaging and re-imaging a diverse set of samples and imaging methods: live mammalian cells at different time points; fixed bacterial cells on two microscopes with different imaging modalities; and nanostructures on optical and electron microscopes. FARMER can be readily adapted to any imaging system with an encoded motorized stage and can facilitate multi-session and multi-platform imaging experiments in biology, materials science, photonics, and nanoscience. Published by AIP Publishing. [<http://dx.doi.org/10.1063/1.4982818>]

I. INTRODUCTION

In many experiments that involve imaging, it is useful or even necessary to locate and relocate specific regions of interest (ROIs) of a sample on different instruments or on the same instrument at different time points before and after an off-platform procedure. For example, nanostructures or biological cells may need to be imaged on an optical microscope (in the first session) for optical properties or information about fluorescently labeled organelles and on an electron microscope (in the second session) for structural details.^{1,2} Specific ROIs (e.g., cells or nanostructures), once imaged in the first session, may need to undergo manipulations not possible on the optical microscope (such as those requiring a sterile environment or involving complex protocols) before being imaged in the

subsequent sessions. Furthermore, since many microscopes are shared resources, samples have to be dismounted to accommodate other experiments before being imaged again. In all of these cases, the specific ROIs need to be relocated. Manually searching for the ROIs, which could be as small as a few microns, is almost always excessively time consuming or sometimes impossible.

The relocation process can be aided by fabricating arrays of features onto the samples, such as grids on commercial coverslips, arrays of metal features,¹ transmission electron microscopy (TEM) grids,² laser carved features,³ numbers on container lids,⁴ and printed patterns taped on the bottom of the samples.⁵ Although useful in particular cases, these approaches might require complex fabrication processes.^{1,4,5} Also, the fabricated features can interfere with the samples by taking up space,^{1,2} and therefore, limit sample volume (a concern for samples containing cells)⁴ or introduce imaging artifacts (e.g., gridded cover slips and some other techniques^{4,5}). Moreover, none of the above approaches allows accounting for sample tilting.

^{a)}T. Huynh and M. K. Daddysman contributed equally to this work.

^{b)}Present address: Intellectual Ventures Laboratory, Bellevue, Washington 98007, USA.

^{c)}Author to whom correspondence should be addressed. Electronic mail: nfschere@uchicago.edu.

In this paper, we describe a method termed Fast and Accurate Relocation of Microscopic Experimental Regions (FARMER) (Fig. 1) that can accurately and precisely relocate ROIs quickly and conveniently. The approach uses the coordinates of 3 (or more) conspicuous reference points (REFs) found in each imaging session and the coordinates of all points (REFs and ROIs) obtained in the first session (Fig. 1(a)). This method enables the accurate and precise determination and relocation of specific ROIs in subsequent imaging sessions, on the same (Fig. 1(b)) or different instrument (Fig. 1(c)). The 3 distinct REFs can be fabricated by hand with simple tools (permanent markers or conductive pens) in regions of the sample or the substrate away from the ROIs, eliminating concerns about complexity in fabrication and interference with the ROIs. Alternatively, the REFs can also be chosen among the ROIs.^{1,6}

The FARMER algorithm calculates geometric operators to match the sets of coordinates of the REFs in the first and second (or subsequent) sessions (Fig. 2(a), Multimedia view). With the operators on the second set inverted, these operators are then arranged in a sequence that transforms the first set of coordinates to the second set (Fig. 2(b), Multimedia view). This sequence of operators is then applied on the coordinates of

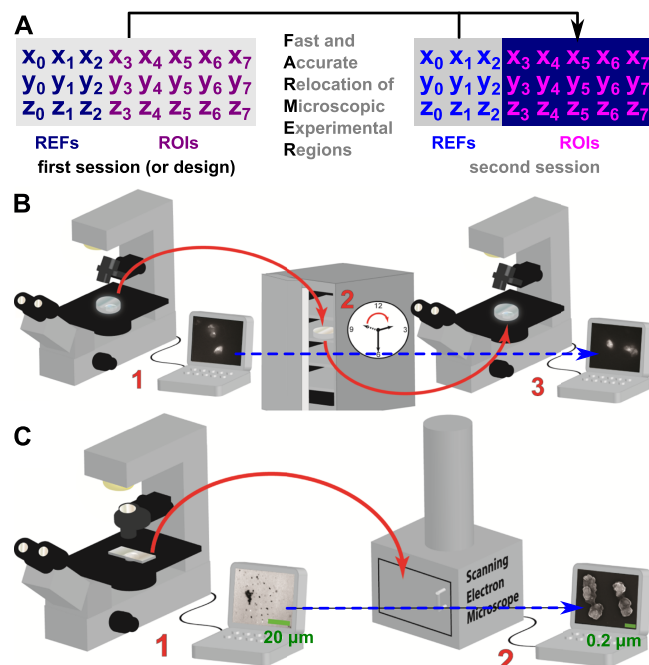


FIG. 1. Summary of the Fast and Accurate Relocation of Microscopic Experimental Regions (FARMER) and example experimental protocols to which FARMER is applied. (a) Schematic describing FARMER. Coordinates of regions of interest (ROIs) in the second imaging session are calculated using all coordinates (reference points, REFs, and ROIs) found in the first session or by design. (b) Schematic depicting imaging at different time points. (b1) An image of live fluorescently labeled cells is obtained at the first time point. (b2) The cell-containing dish is incubated for a period of time in a specific incubator. (b3) FARMER is then used to quickly relocate and image the same cells at a second time point. (c) Schematic depicting imaging across platforms. (c1) A pattern of metal nanoparticles is imaged using optical microscopy at low magnification. (c2) The sample containing the nanoparticles is then transferred to a scanning electron microscope (SEM). FARMER is then used to quickly relocate the same pattern, allowing the user to image at much higher resolution to obtain structural details, such as the arrangement of nanoparticles in a cluster.

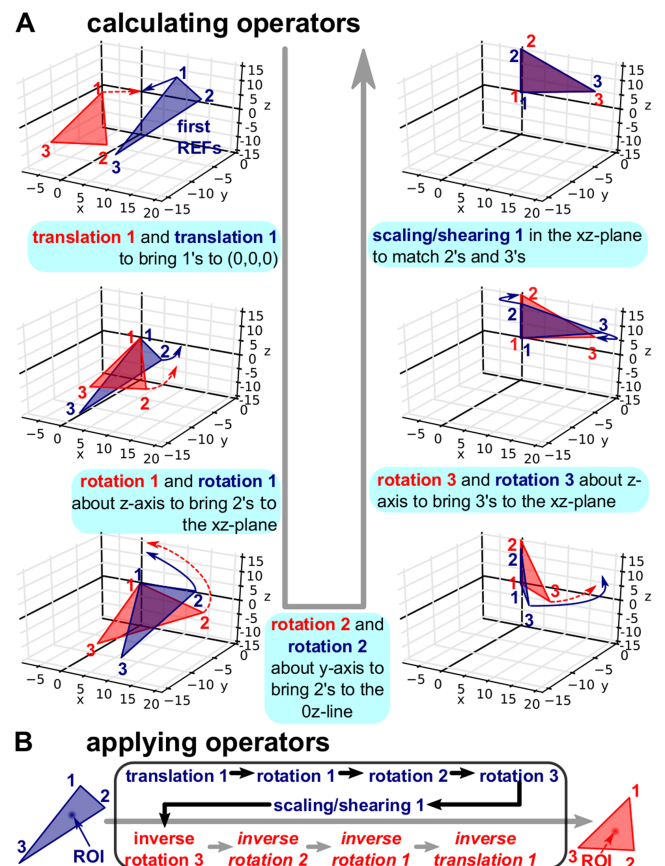


FIG. 2. Schematic explaining the FARMER algorithm. The goal is to transform the first set of REF and ROI coordinates (blue) to the second set of REF and ROI coordinates (red). (a) Schematic explaining how the geometric operators are found. Both sets of coordinates are moved onto the xz-plane, with REF1s at the origin and REF1-REF2 sides on the z-axis, by translation and rotation. To account for possible errors in coordinate recording, a shearing/scaling operator (Equation (1)) is applied to the first set, matching it completely to the second set. The operators are calculated and recorded. (b) Schematic explaining the application of the geometric operators found in (a). The geometric operators for the first set (blue) and the inverse of those for the second set (red) are applied on the first set of ROI coordinates to find the new ROI coordinates. (Multimedia view) [URL: <http://dx.doi.org/10.1063/1.4982818.1>] [URL: <http://dx.doi.org/10.1063/1.4982818.2>]

the ROIs in the first session to find the coordinates of the ROIs in the second session. The geometric operators are translation, z- and y-axis rotation, and scaling/shearing in the xz-plane (Equation (1)),

$$\begin{aligned} z\text{-axis rotation} &= \begin{bmatrix} \cos(\theta) & -\sin(\theta) & 0 \\ \sin(\theta) & \cos(\theta) & 0 \\ 0 & 0 & 1 \end{bmatrix}, \\ y\text{-axis rotation} &= \begin{bmatrix} \cos(\phi) & 0 & \sin(\phi) \\ 0 & 1 & 0 \\ -\sin(\phi) & 0 & \cos(\phi) \end{bmatrix}, \\ \text{scaling/shearing} &= \begin{bmatrix} s_x & 0 & 0 \\ 0 & 1 & 0 \\ s_z k_z & 0 & s_z \end{bmatrix}. \end{aligned} \quad (1)$$

The scaling/shearing operator is used to account for errors in recording the coordinates (caused by both the user and the

stage) and possible discrepancies in units in the first and subsequent sets of coordinates. The operations are performed in 3-dimensional (3D) space and thus can correct for arbitrary tilting and rotation.

We characterized the accuracy and precision of the FARMER method with a control experiment that also represents a typical imaging experiment (Figs. 3 and 4). We illustrate the versatility and general applicability of the FARMER method with several actual experiments involving several samples and imaging methods. In the first of these, the same live adherent cultured cells were re-imaged after the dish had been removed and repositioned on the microscope (Fig. 5). In the second example, the same fixed bacteria were imaged sequentially on a home-built multifocal microscope (MFM)⁷ and a confocal microscope (Fig. 6). The third example involves imaging specific structures of Ag nanoparticles fabricated using laser tweezers on an optical microscope⁸ before being imaged on a scanning electron microscope (SEM) for structural details (Fig. 7).

II. EXPERIMENTAL SETUPS

A. Sample preparation and imaging to characterize the accuracy and precision

A permanent marker (Sharpie, black Ultra-Fine) was used to draw the REFs (X's) on a number-0 cover slip. Typically, we use X's but other crossing features also work. For convenience in handling, the cover slip was attached to a glass slide (1 in. × 3 in.) using Norland Optical Adhesive 81, with the REFs facing the glass slide. Images were taken with a digital camera (Olympus PEN), a stereoscope (Leica GZ7), and a bright field microscope (Olympus UPlanSApo 100x/1.40 oil objective). A micro-stage (Ludl Electronics Products, 99S108-O2-LE, Serial 144823) was used for positioning.

B. Preparation and imaging of the sample containing live mammalian cells

Insulin secreting MIN6 cells⁹ (passage 25) were cultured in glass-bottom dishes (MatTek P35G-0-14-C), in high-glucose DMEM (Life Technologies 10569), supplemented with fetal bovine serum (10%, Life Technologies 10437), and penicillin-streptomycin (100 U/ml, Life Technologies 15140), under standard atmosphere (5% CO₂, 37 °C). The cells were fluorescently labeled by transfection with Lipofectamine 2000 (Life Technologies 11668) and insulin-C-peptide-GFP plasmid¹⁰ (4 µg DNA + 10 µl reagent/250 µl un-supplemented DMEM). The REFs were made with a permanent marker (Staedtler 318-3). The imaging was done on a spinning-disk confocal microscope (Olympus DSU on IX-81 microscope, Objective: Olympus UPlanSApo 100x/1.40 oil immersion, Stage: Prior ProScan II H117P1I4).

C. Preparation and imaging of the sample containing fixed bacteria

Pseudomonas fluorescens (SBW25) bacteria tagged with mNeonGreen¹¹ were provided by Prof. Mark Bailey (Centre

for Ecology and Hydrology, UK) via Dr. Rosemarie Wilton (Argonne National Laboratory, USA). Fresh bacteria were grown by transferring a colony from an agar plate with a 1 µl sterile loop to 5 ml of nutrient broth and grown in the dark for 10 h at room temperature. Subsequently, 300 µl of the cell suspension was mixed with 300 µl of 2x fixing buffer¹² (100 mM KP_i, 2 mM MgCl₂, fresh 8% formaldehyde, and fresh 0.50% glutaraldehyde, pH 6.5, Electron Microscopy Sciences) and stored on ice for 60 min. The fixed bacteria were washed 3 times. Each wash involves centrifuging (1500 g for 2 min), removing the supernatant, and resuspending with 300 µl cold phosphate-buffered saline (PBS) (Hyclone Laboratories SH30256.01). After the final wash, the cells were re-suspended in 100 µl of PBS and stored in the dark at 4 °C. To prepare the samples for imaging on the multifocal microscope (MFM),⁷ 1 µl of bacteria suspension was pipetted into a 1.5-ml tube and diluted with 9 µl of PBS. A 1 µl aliquot of the diluted bacterial suspension (~200 bacteria/nl) was pipetted onto a 170 µm thick (No. 1.5) glass coverslip. Three REFs (X, +, and T) were made on the coverslip using a permanent marker (Sharpie Ultra-Fine). The coverslip was mounted on a microscopy glass slide and sealed with nail polish. The image of the coverslip with REFs was taken with a digital camera (Samsung Galaxy S4), and the white balanced was corrected using ImageJ.

The MFM consists of a 60x NA 1.27 water immersion objective (Nikon 60x 1.27 NA PlanApo IR water immersion, MRD07650) on a Nikon Eclipse Ti with a mechanical stage (Ludl 99S106-N2K-LE2, controller MAC5000). The MFM optic was custom made in-house and positioned in a 4-f optical system extending from the camera port of the inverted microscope. The 4-f lenses provide an additional 2x magnification. The MFM images were detected using an Andor iXon Ultra 888 EMCCD. The excitation light was provided by the Cyan channel of a Spectra X light engine (Lumencor).

The MFM diffractive optic was designed with an undistorted pitch of 91 µm and a focal shift Δz = 250 nm, using previously developed formulas.⁷ The fabrication on a 5 mm thick UV fused silica substrate (Thorlabs WG41050) was completed at the Pritzker Nanofabrication Facility at the University of Chicago.

Data acquisition by confocal microscopy was performed using a Yokogawa W1 spinning disk confocal attached to a Nikon Eclipse Ti with a Prior stage (Prior ProScan H117E1N5/F, controller H31XYZ7EF). A 100x 1.45 NA oil immersion objective (Nikon 100x NA 1.45 PlanApo oil immersion, MRD01905) was used. The detection was done with an Andor iXon Ultra 888 EMCCD. The excitation light was provided by a 488 nm CW laser (Spectra-Physics Excelsior One 488C-100). The system was controlled with Micro-manager software.¹³

D. Preparation and imaging of the pattern of metal nanoparticles

The pattern of Ag nanoparticles on a glass cover slip was fabricated by “optical printing” using an optical tweezer apparatus as described previously.⁸ Imaging was performed on a LabRAM HR Evolution optical microscope (Horiba,

Olympus MPlanN 10x/0.25 and MPlanN 100x/0.90 objectives) and a FEI Nova NanoSEM 230 instrument. Each REF was made by drawing a thick line with a conductive pen (Circuit Works CW2000), letting the ink dry, then drawing a metal needle through the thick line to generate sharp features. The ink, a suspension of Ni particles, is visible (i.e., gives contrast) in both the light and electron microscopes.

III. RESULTS

We used a test REF/ROI sample to demonstrate the FARMER method's general capabilities. The REFs were created with a permanent marker and the ROIs were (re-)located despite sample rotation and tilting. We drew 16 X's on a coverslip in a 4×4 array, then glued the cover slip to a glass slide (the side with X's faces the glass slide) (Fig. 3(a)). The 16 positions were numbered from 0 to 15 (left to right, top to bottom); and positions 0, 3, and 13 were chosen as REFs while the rest were treated as ROIs. While the X's were quite large with each stroke spanning ~ 3 mm, the acute angles of intersection between the two strokes remained sharp at higher magnification even at 100x (Figs. 3(b) and 3(c)). In principle, one may

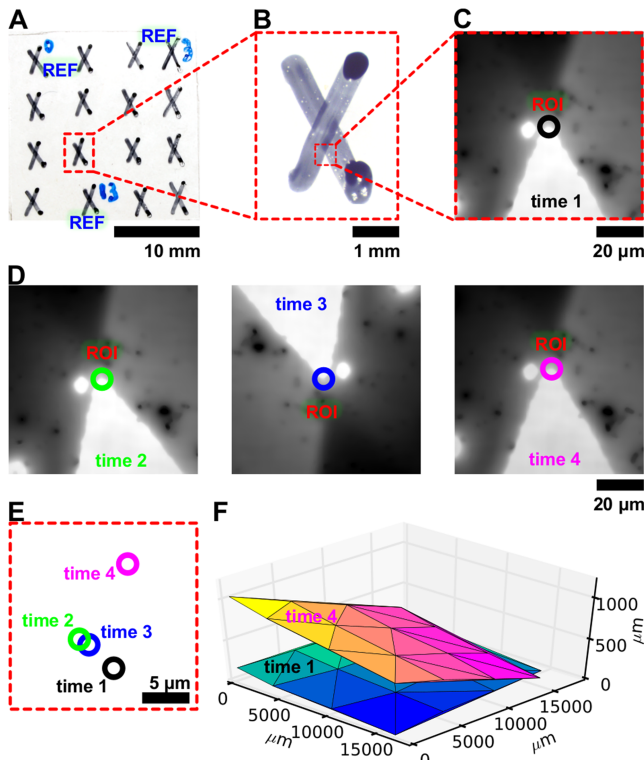


FIG. 3. Demonstration of rapid relocation using FARMER. The test sample contains regions of interest (ROIs) and reference points (REFs) made with a permanent marker. (a) Picture of the test sample taken with a digital camera. Sixteen X's were drawn with a permanent marker on a coverslip, which was then glued to the bottom of a glass slide. Three ROIs are chosen as REFs as specified. (b) Image of a whole letter X taken with a stereoscope. (c) Microscope image of a ROI, which is a vertex of the angle of intersection between the strokes in the letter X. (d) Images of the same ROI in (b) at subsequent time points. Before each time point, the sample was removed from the stage and remounted with deliberate rotation and tilting. (e) Plot showing the positions of the ROI in (b) at different time points in the recorded images. (f) Plot of the ROI/REF coordinates at time point 1 and time point 4 showing deliberate tilting (approximately 1-mm difference in focus at one corner of a 1.5-cm square).

use any shape, besides an X (e.g., Fig. 6(a)), as a REF as long as it provides an easily recognizable feature at the desired magnification. In the first imaging session, we found the coordinates of the REFs and ROIs, defined as the vertices of the lower acute angle formed where the strokes meet (Fig. 3(c)). In each of the subsequent sessions, the ROIs were rapidly relocated using FARMER (Fig. 3(d)) (~ 3 min/session). The relocation was successful (Fig. 3(e)) even with deliberate rotating and tilting of the sample (Fig. 3(f)).

We characterized the accuracy and precision of the FARMER method for the handmade test sample (Fig. 3) through six relocation experiments on a microscope with a 100x objective, with deliberate rotation and tilting each time. The error of relocation of an ROI in an experiment was defined as the distance between the two vertices of the bottom acute angle of the X's when the picture in the first session is overlaid with the picture in a subsequent session (Figs. 3(c) and (d)). The aggregated data (6 relocation experiments, 16 positions/experiment, including user errors in relocating REFs) yielded errors of $-1.25 \pm 3.41 \mu\text{m}$ and $0.04 \pm 2.86 \mu\text{m}$ in the X-axis and Y-axis, respectively (Fig. 4(a)). The individual average error at each position could be as small as $2 \mu\text{m}$ (Fig. 4(b)), and in 94% of the cases the error was smaller than $8 \mu\text{m}$ (Fig. 4(c)) with larger errors occurring at the edges away from the reference points. We consider the errors from

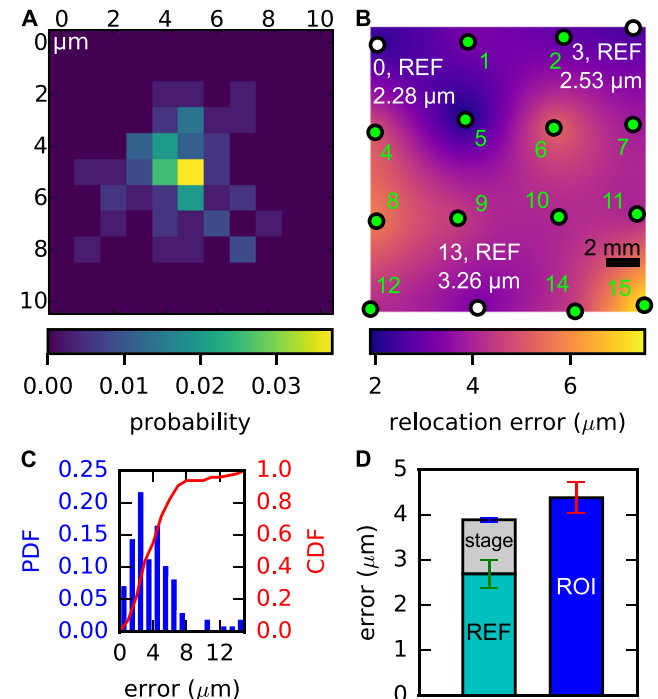


FIG. 4. Characterization of accuracy and precision. (a) 2D histogram (X, Y-axes) of the errors aggregated from 6 relocation experiments of 16 positions (96 points). The images were obtained with a 100x oil immersion objective. (b) Color map of average errors (distances) in relocating the regions of interest (ROIs) (six trials). The error is the average shift required to align the relocated image with the original image taken at that coordinate. The user errors are those at the reference points (REFs), positions 0, 3, and 13. The heat map was generated by linear interpolation. (c) Plots of the probability density function (PDF, bars) and the cumulative distribution function (CDF, line) of all the errors of relocation. (d) Bar chart of the mean error at the ROIs ($4.38 \pm 0.34 \mu\text{m}$, $N = 78$), at the REFs ($2.69 \pm 0.30 \mu\text{m}$, $N = 18$), and by stage movement ($1.20 \pm 0.05 \mu\text{m}$, $N = 75$). The error bars indicate standard errors for the ROIs.

manually locating the REFs to the centers of the fields of view as the standard for comparison. With this in mind, the average error at the ROIs (FARMER algorithm) was only $1.69\text{ }\mu\text{m}$ larger than that of the REFs (operator error; e.g., improper repositioning of the sample) (Fig. 4(d)).

The error due to the re-positioning precision of the mechanical stage will also influence FARMER results. To characterize this error, we performed an experiment in which the sample stayed mounted throughout, and the stage moved through the 16 ROI positions in six cycles of relocation. The average error due to stage reproducibility was $1.20\text{ }\mu\text{m}$ (Fig. 4(d)), which would contribute to both the REF and ROI errors. Therefore, FARMER is accurate and precise for most practical purposes. The method reproducibly relocated ROIs, and the individual errors at the ROIs were a few μm , which is much smaller than the field of view even at 100x magnification ($\sim 50\text{ }\mu\text{m}$ wide on the setup used for this experiment).

We investigated the applicability of the FARMER method to imaging a fluorescent biological sample.¹⁴ After taking images of arbitrarily selected MIN6 cells (fluorescent confocal microscopy, 100x objective) at the first time point (i.e., the first session), we relocated the same cells at 2 subsequent time points (30–40 min apart) using FARMER. We also introduced large angles of rotation between each time point (Figs. 5 and S1 of the [supplementary material](#)). The cells were cultured in a glass-bottom Petri dish and transfected to label the insulin granules with GFP. The transfection is only ~20% effective; therefore, the individual cells are selected out of a dense sample (Fig. S1 of the [supplementary material](#)). Each of the 3 REFs was made by drawing an X (~3 mm long) on the bottom of the glass area in the dish (similar to those made for the test sample, Fig. 3). In the first imaging session, the 3 REFs and 5 cell-containing ROIs were found using a confocal microscope (Fig. 5(a)). Each REF coordinate was determined by focusing on and centering the intersection of the X (Fig. 5), followed by moving to the common focal plane of the cells (Fig. 5(c)). Even though the dish was dismounted and remounted with deliberate large rotations and significant tilting (indicated by differences in focus as large as 1 mm at one corner of a 1.5-cm square) in two subsequent imaging sessions, the cells were easily relocated with FARMER and imaged (Figs. 5(d) and S1 of the [supplementary material](#)). Each relocation process took 3–5 min.

We demonstrate the cross-platform capability of FARMER using bacteria imaged on different optical microscopes with different imaging modalities. The specimen consisted of fluorescent bacteria (*Pseudomonas fluorescens*, strain SBW25, expressing unconjugated mNeonGreen)¹¹ that were mounted on a glass coverslip via chemical fixation. Among many groups of bacteria, six groups were selected for imaging based on their unique shapes, so that we were certain the same bacteria were imaged on two different microscopes. The groups were first imaged on a home-built widefield epifluorescent multifocal microscope (MFM), then transferred to and imaged on a spinning-disk confocal microscope. An experienced optical microscopy operator attempted and failed to relocate the bacteria on a confocal microscope without FARMER after >8 h of effort. By contrast, the FARMER relocation

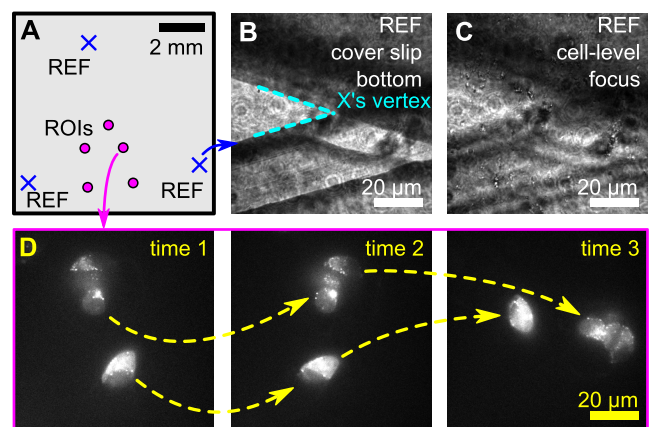


FIG. 5. Relocation of biological cells using FARMER in subsequent imaging sessions using optical confocal microscopy at high magnification (with a 100x objective). (a) Plot showing positions of the ROIs and REFs in the first imaging session (time 1). (b) Bright field image of a REF made by a permanent marker, focused at the bottom of the coverslip. (c) Bright field image of the REF in (b), focused at the top of the coverslip. The REF is defined as the vertex of the angle of intersection between the strokes in the letter X, similar to the REFs/ROIs in the test device (Fig. 3). (d) Fluorescence confocal images of a ROI at three different time points, obtained after using FARMER to take images at time 2 and time 3. The same cells were relocated even with deliberate shifts and rotations. The results for all cells are shown in the [supplementary material](#) (Fig. S1).

procedure (after the first imaging session) took less than 30 min! The full FARMER relocation procedure included the following steps: remounting the specimen on the confocal microscope, locating the REFs (Fig. 6(a)), generating new coordinates, and acquiring a z-series of fluorescent at the calculated coordinates (80 z-planes at 50 nm spacing). One example (Fig. 6(b) and 6(c)) shows that FARMER was able to relocate the same group of bacteria despite large differences in sample orientation (Fig. S3 of the [supplementary material](#)) and magnification when imaging on the two microscopes. This group of bacterial cells was chosen as it has a unique, identifiable bacteria cluster structure. The relocation was accurate—the group was visible after moving the stage to the coordinates provided by FARMER—and only a small amount of fine tuning was required to center the group in the field of view. The FARMER method enables such multi-modal experiments, and, in this particular case, helped verify the optical properties of the home-built MFM setup.

The cross-platform capability of FARMER was further demonstrated by imaging a sample of patterned metal nanoparticles using both optical microscopy and scanning electron microscopy (SEM). The ROI was a pattern of Ag nanoparticles made by optical printing,⁸ surrounded by 3 REFs (Fig. 7(a)). The goal was to image the detailed structure of the pattern of nanoparticles on a range of scales. Optical microscopy can reveal the pattern on a large scale (1–100 μm) but is diffraction-limited (Fig. 7(b)) and unable to resolve structure on the nanoscale. To image at higher resolution on different instruments, such as an SEM, a key issue is to be able to rapidly locate the small and sparse ROI. Normally, a manual search takes ~2 h by an operator with extensive expertise in SEM imaging. Furthermore, even when the ROI was in the field of view, both higher magnification and averaging over more

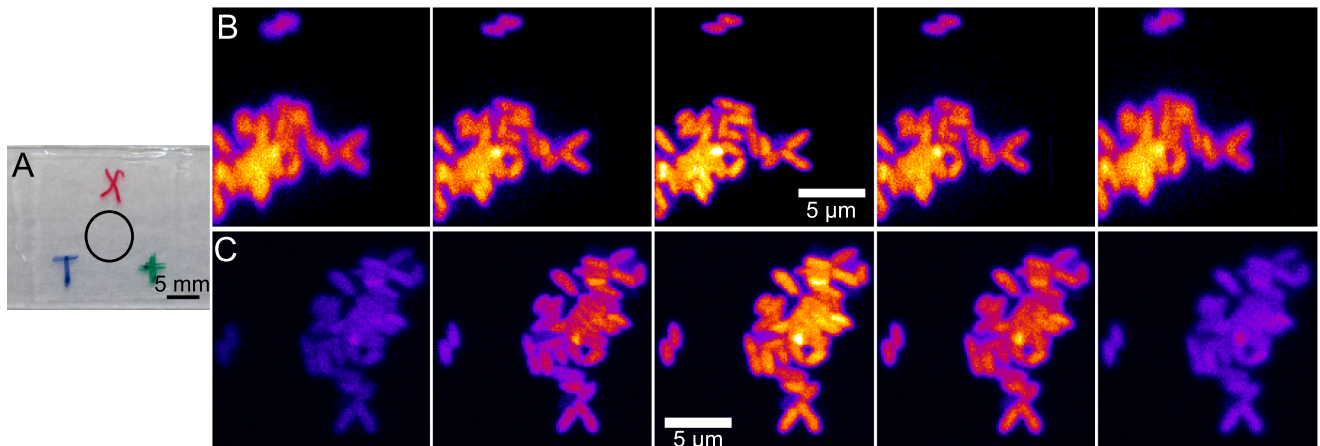


FIG. 6. Relocation of a bacteria on a confocal microscope after imaging on a multifocal microscope (MFM). (a) Picture of the coverslip sample. The images in panels (b) and (c) were taken from inside the black ring overlaid on the image. FARMER relocation REFs were the red “X,” green “+,” and blue “T.” The right angle intersections in the “+” and “T” were more difficult to localize than the acute angle of the “X” intersection; however, the shapes worked adequately for FARMER. The colors are another method of identifying the different REFs to image them in the same order on each microscope. (b) Images in a z-series of fixed *Pseudomonas fluorescens* (SBW25) bacteria taken with a home-built widefield epifluorescent multifocal microscope. This particular group of bacteria was chosen to demonstrate the FARMER method because of the unique grouping of the bacteria in the dense sample. For simplicity, this figure includes only 5 z-planes out of the 25 z-planes collected simultaneously by the MFM. (c) Images in a z-series of the same bacteria described in (b) obtained with a confocal microscope after imaging with the MFM. The FARMER method was used to relocate the bacteria after the specimen was transferred to the confocal microscope. Note that the bacteria image is the same shape and size after accounting for the changes in magnification and specimen orientation (90° rotation and flipping, Fig. S3 of the [supplementary material](#)). We left the images in (b) and (c) rotated from each other as this is how they appeared on the detector of each microscope. The confocal images were cropped to the same number of pixels as the MFM field of view (from a full 1024 pixel square) and z-planes were selected to correspond to the same z-planes in B (out of 80 z-planes at the 50 nm spacing). In panels (b) and (c): z-plane spacing: 0.25 μm . The lookup table is ImageJ Fire.

scans were required to see it (Fig. 7(c)), making the manual search much harder and slower. The REFs were made similarly as previously described above except with a conductive pen and thus were visible in both the optical microscope and

the SEM. Better spatial accuracy was achieved for each REF by creating a sharp feature formed by drawing a sharp metal needle crossing a nearly dried thick line made by a conductive pen (Figs. 7(b) and 7(c)). Using the FARMER method, we found all the REFs, calculated the coordinates of the ROI, and moved the ROI into the field of view after only 10 min on the SEM (Fig. 7). This is 10-fold faster than a typical manual search! Higher-resolution images reveal the multiscale organization of the particles as expected from the fabrication that had been performed⁸ (Fig. 7(d)).

IV. DISCUSSION

There are important points about the FARMER algorithm (Fig. 2) (Multimedia view) that should be noted. While positioning REFs at different focal planes and skipping the scaling/shearing step introduce small errors, one has to make sure that the handedness of the coordinate system in the algorithm (right-handed as reported) matches those in the instruments (Fig. S2 of the [supplementary material](#)). Furthermore, one can improve the accuracy and precision using sets of coordinates over different sessions (instead of just 1 set) or using more than 3 REFs. With respect to the time required for initial localization and relocation (i.e., in the first session), the rate-limiting step of the method is finding the REFs. The time we spent finding each REF ranged from less than 1 min to 9 min, depending on the user’s familiarity with the sample and the prominence of the REF. The time can be improved further by estimating the locations of the second and third REFs from the image of the first REF. The true locations of the second and third REFs can be confirmed by the user after moving to the estimated location of the second and third REFs.

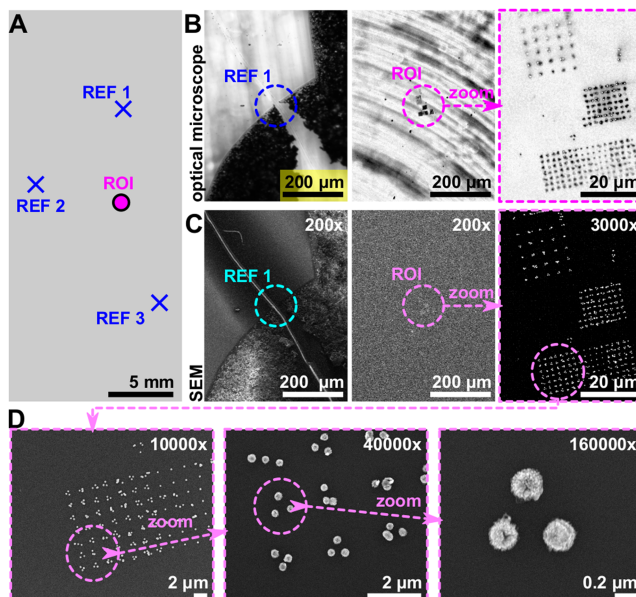


FIG. 7. Relocation of nanometer-scale structures in scanning electron microscopy (SEM) after imaging with optical microscopy. (a) Plot showing positions of the ROI and REFs. (b) Optical images of REF 1 and the ROI taken with the optical microscope. The image at the higher magnification was obtained with a 100x objective. (c) SEM images of REF 1 and the ROI. It took about 9 min to find the ROI with FARMER. Note that with the SEM, the image of the ROI has very low contrast without zooming in and long averaging. (d) Progressively higher-resolution SEM images showing the multiscale organization. Magnifications and scale bars are shown in each panel.

A motorized and encoded stage that can report coordinates and the relative units in each dimension is necessary to perform FARMER. For this work, we used typical stages that can be found in home-built and commercial instruments (Table S1 of the [supplementary material](#)). Integration with the microscope control software is also important to improve the user's experience. We were able to integrate the FARMER script written in Python with microscope/stage controlling programs we wrote in LabVIEW, Matlab, and Micro-manager. Using the FARMER script with proprietary programs was also possible but not as convenient due to the lack of access to the source code. Software programs may be developed to interface with the FARMER Python script (e.g., via text files) or incorporate FARMER via the native language (e.g., Java in Micro-manager).

An advantage of the FARMER method is the ease of REF fabrication, which requires only a permanent marker or a conductive pen. These simple markings are sufficient in most cases of optical and SEM imaging, but these could be improved upon. REFs created by permanent markers have limited durability due to their solubility in objective immersion oil (or other organic solvents) and sensitivity to mechanical abrasion. For cell culture and imaging, a solution would be to glue the REF-containing cover slip to a plastic dish with a hole, with the REFs between the glass and the plastic (similar to the test device we made above in Fig. 3). The liquid-based conductive pen used in this work produces very thick features. While sharp features used as REFs can be made by using a needle to cut the thick feature (Fig. 7(b)), a conductive pen that gives the same consistency as a permanent marker would be a more direct tool. Previously developed techniques^{1,2,4,5} could also be used, with a much reduced demand on fabrication.

V. CONCLUSIONS

The FARMER method enables simple, fast, accurate, and precise relocation of ROIs across instruments and time points, even with sample rotation and tilting. ROI location and relocation are done rapidly, at least 10-fold faster than manual searches. It is compatible with different sample types (cells, nanostructures, hand drawn reference marking, etc.). The reference points are made by simple hand fabrication with common tools (permanent markers and conductive pens). FARMER enables comparative measurements and can be readily adapted to any experimental imaging system with a motorized stage and the capability to locate the reference points.

The three applications demonstrated here (live mammalian cells, Fig. 5, fixed bacterial cells, Fig. 6, and nanostructures, Fig. 7) represent two common classes of samples with potentially complex imaging needs, biological systems and synthetic materials. The FARMER method can be extended to imaging other biological systems (from cells to organisms) on traditional platforms or in microfluidic devices containing a large number of samples,^{15–18} to monitor their dynamics over long duration studies. With this method, multi-platform imaging of nanostructures can be readily performed, allowing one to obtain detailed structural information (e.g., via electron microscopy) to complement optical information

(including spectroscopic data).^{19–21} Monitoring microfluidic reactions²² and crystallization²³ would also benefit from this method.

SUPPLEMENTARY MATERIAL

See [supplementary material](#) for the following items:

- Supplementary text.
- Python script and example input/output files: Relocation.py, Original.txt, Input.txt, REFIndex.txt, and Output.txt.

ACKNOWLEDGMENTS

We thank Rustem F. Ismagilov, Elena M. Luchetta, Rebecca R. Pompano, Christopher B. Huppenbauer, and Justin E. Jureller for technical help and suggestions in the initial development of the method. We thank Rosemarie Wilton and Mark Bailey for the gift of labeled bacteria. We acknowledge the University of Chicago NSF Materials Research Science & Engineering Center (MRSEC) and the NanoBiology Facility at the University of Chicago for instrumental and general facilities support. This work made use of the Pritzker Nanofabrication Facility of the Institute for Molecular Engineering at the University of Chicago, which receives support from SHyNE, a node of the National Science Foundations National Nanotechnology Coordinated Infrastructure (No. NSF NNCI-1542205). We also thank the W. M. Keck Foundation, NSF-MRSEC (DMR-0820054), and the U.S. Department of Energy (Contract No. DE-AC02-06CH11357) for funding. M.K.D. was supported by a Yen Fellowship from the Institute for Biophysical Dynamics at the University of Chicago.

¹R. Jin, J. E. Jureller, and N. F. Scherer, *Appl. Phys. Lett.* **88**, 263111 (2006).

²M. Bhave, E. Papanikou, P. Iyer, K. Pandya, B. K. Jain, A. Ganguly, C. Sharma, K. Pawar, J. Austin, K. J. Day, O. W. Rossanese, B. S. Glick, and D. Bhattacharyya, *J. Cell Sci.* **127**, 250 (2014).

³I. Kolotuev, Y. Schwab, and M. Labouesse, *Biol. Cell* **102**, 121 (2010).

⁴L. Hanson, L. Cui, C. Xie, and B. Cui, *Microsc. Res. Tech.* **74**, 496 (2011).

⁵K. Yun, J. Chung, Y. Park, B. Lee, W. G. Lee, and H. Bang, *Anal.* **138**, 3196 (2013).

⁶R. Jin, J. E. Jureller, H. Y. Kim, and N. F. Scherer, *J. Am. Chem. Soc.* **127**, 12482 (2005).

⁷S. Abrahamsson, J. Chen, B. Hajj, S. Stallinga, A. Y. Katsov, J. Wisniewski, G. Mizuguchi, P. Soule, F. Mueller, C. Dugast Darzacq, X. Darzacq, C. Wu, C. I. Bargmann, D. A. Agard, M. Dahan, and M. G. L. Gustafsson, *Nat. Methods* **10**, 60 (2013).

⁸Y. Bao, Z. Yan, and N. F. Scherer, *J. Phys. Chem. C* **118**, 19315 (2014).

⁹H. Ishihara, T. Asano, K. Tsukuda, H. Katajiri, K. Inukai, M. Anai, M. Kikuchi, Y. Yazaki, J. I. Miyazaki, and Y. Oka, *Diabetologia* **36**, 1139 (1993).

¹⁰S. Rajan, S. C. Eames, S.-Y. Park, C. Labno, G. I. Bell, V. E. Prince, and L. H. Philipson, *Am. J. Physiol.: Endocrinol. Metab.* **298**, E403 (2010).

¹¹M. J. Bailey, A. K. Lilley, I. P. Thompson, P. B. Rainey, and R. J. Ellis, *Mol. Ecol.* **4**, 755 (1995).

¹²O. W. Rossanese, C. A. Reinke, B. J. Bevis, A. T. Hammond, I. B. Sears, J. O'Connor, and B. S. Glick, *J. Cell Biol.* **153**, 47 (2001).

¹³A. D. Edelstein, M. A. Tsuchida, N. Amodaj, H. Pinkard, R. D. Vale, and N. Stuurman, *J. Biol. Methods* **1**, 10 (2014).

¹⁴S. M. A. Tabiei, S. Burov, H. Y. Kim, A. Kuznetsov, T. Huynh, J. Jureller, L. H. Philipson, A. R. Dinner, and N. F. Scherer, *Proc. Natl. Acad. Sci. U. S. A.* **110**, 4911 (2013).

- ¹⁵H. Hwang and H. Lu, *Biotechnol. J.* **8**, 192 (2013).
- ¹⁶K. Chung, C. A. Rivet, M. L. Kemp, and H. Lu, *Anal. Chem.* **83**, 7044 (2011).
- ¹⁷M. Mehling and S. Tay, *Curr. Opin. Biotechnol.* **25**, 95 (2014).
- ¹⁸G. Grossmann, W.-J. Guo, D. W. Ehrhardt, W. B. Frommer, R. V. Sit, S. R. Quake, and M. Meier, *Plant Cell* **23**, 4234 (2011).
- ¹⁹J. R. Kirschbrown, R. L. House, B. P. Mehl, J. K. Parker, and J. M. Papanikolas, *J. Phys. Chem. C* **117**, 10653 (2013).
- ²⁰M. M. Gabriel, J. R. Kirschbrown, J. D. Christesen, C. W. Pinion, D. F. Zigler, E. M. Grumstrup, B. P. Mehl, E. E. M. Cating, J. F. Cahoon, and J. M. Papanikolas, *Nano Lett.* **13**, 1336 (2013).
- ²¹B. P. Mehl, J. R. Kirschbrown, M. M. Gabriel, R. L. House, and J. M. Papanikolas, *J. Phys. Chem. B* **117**, 4390 (2013).
- ²²W. Liu, D. Chen, W. Du, K. P. Nichols, and R. F. Ismagilov, *Anal. Chem.* **82**, 3276 (2010).
- ²³L. Li, W. Du, and R. F. Ismagilov, *J. Am. Chem. Soc.* **132**, 112 (2010).